Thermal Analysis of a Magnetic Induction Thruster

C. J. Zang* and M. M. Micci†
The Pennsylvania State University, University Park, Pennsylvania

The thermal behavior of a magnetic induction thruster utilizing a solid conducting ring as the reaction mass is analyzed. Electrical energy initially stored in a capacitor is discharged through a coil in close proximity to the reaction mass. Opposing magnetic fields subsequently accelerate the reaction mass to a high exit velocity. During the acceleration process, the reaction mass is resistively heated and the effects of the varying temperature-dependent electrical conductivity, specific heat, and density are analyzed and compared to the constant property case. The effects of thruster geometry and reaction-mass phase changes are also examined.

Nomenclature

C = capacitance
C_P = specific heat
F = force
I = current
L = self inductance
m = mass
M = mutal inductance
MW = gram-molecular weight
N = number of drive-coil turns
P = pressure
R = resistance
t = time
T = temperature
V = voltage
W = evaporation rate
x = axial distance

Introduction

THE principle of pulsed inductive electromagnetic acceleration has been applied to advanced space propulsion since the 1960s. Its feature is the absence of electrodes in contact with the reaction mass, thereby eliminating electrode erosion concerns. Pulsed inductive thruster operation is diagrammed in Fig. 1. Electrical energy usually stored in a capacitor is discharged through a coil in close proximity to a reaction mass. While the current in the driver coil is rising, it induces an opposite current in the reaction mass (assuming sufficient conductivity) and the opposing magnetic fields generated by the two current loops accelerate the coils in opposite directions. The most notable success with these devices has been achieved by Lovberg and Dailey[1] utilizing a flat, 1-m-diam coil and argon gas as the propellant. They measured specific impulses up to 2240 s and efficiencies up to 50%. One of the major loss mechanisms associated with this device is the energy needed to ionize the argon to obtain sufficient electrical conductivity before acceleration can begin. This ionization energy is lost in the exhaust.

In 1981, Mongeau and Kolm[2] suggested the use of solid conducting material as the reaction mass. Since the reaction mass is already electrically conductive, no energy input is needed prior to acceleration. Both analytical and experimental results obtained by Mongeau and Kolm[3] and Mongeau[4] indicated that such a device could achieve high efficiencies and thrust levels at moderate specific impulses (~1000 s). Experiments by Bondaletov and Ivanov[5] with a geometrically similar accelerator have achieved exhaust velocities up to 5000 m/s. When the data of Refs. 2-5 are displayed together (Fig. 2) it can be seen that the exhaust velocity scales proportionally with one-tenth of the initial capacitor voltage. It was unknown whether the same proportionality would hold as the exhaust velocity is increased from 5 to 10 km/s. The analysis by Mongeau did not take into account the heating of the reaction mass due to the induced currents or the change in material properties resultant from the temperature rise. It was anticipated that, as the capacitor voltage was increased, resistive heating effects would become more dominant. This analysis was initiated to examine the effects of resistive heating and temperature-dependent reaction-mass properties on a pulsed inductive thruster utilizing a solid conducting ring as the reaction mass.

Governing Equations

The pulsed inductive thruster/reaction-mass system elements are modeled as shown in Fig. 3. Electrical energy is stored in the capacitance, C. L_0 and R_0 are the self inductance and resistance, respectively, of the driver circuit. L_1 is the self inductance of the driver coil and L_2 is the self inductance of the current loop which is induced in the reaction mass, while M_{12} is the mutual inductance between L_1 and L_2. The electrical resistance of the reaction mass, which herein was allowed to be a function of temperature, is designated by R_2. I_1 and I_2 are the currents in the driver circuit and reaction mass, respectively. This study began looking at the acceleration of small metallic spheres until calculations of the skin depth and mutual inductance indicated that current would be induced only in the outer periphery of the reaction mass. Thus, the spheres were replaced by rings with cross-sectional radii on the order of the skin depth at the initial reaction-mass temperatures (< 1 mm). As the reaction mass is heated its conductivity decreases, increasing the skin depth. The axial force acting to accelerate the reaction mass can be obtained from the derivative of the magnetic potential energy with respect to the axial direction.

$$F = I_1 I_2 \frac{dM_{12}}{dx} \tag{1}$$

The derivative of M_{12} is a function of the thruster geometry, reducing the problem to one of calculating I_1 and I_2, obtained

Received Feb. 8, 1985; revision received Aug. 20, 1985.

*Undergraduate Research Assistant, Department of Aerospace Engineering. Currently Member of Technical Staff, Hughes Aircraft Company, El Segundo, CA. Student Member AIAA.

†Assistant Professor, Department of Aerospace Engineering. Member AIAA.

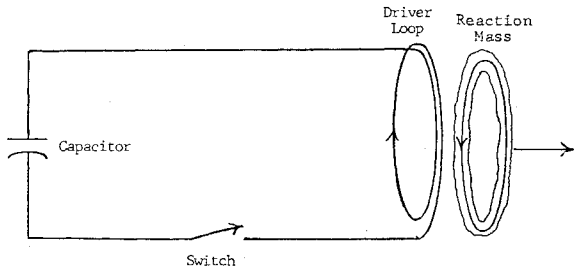

Fig. 1 Pulsed inductive thruster.

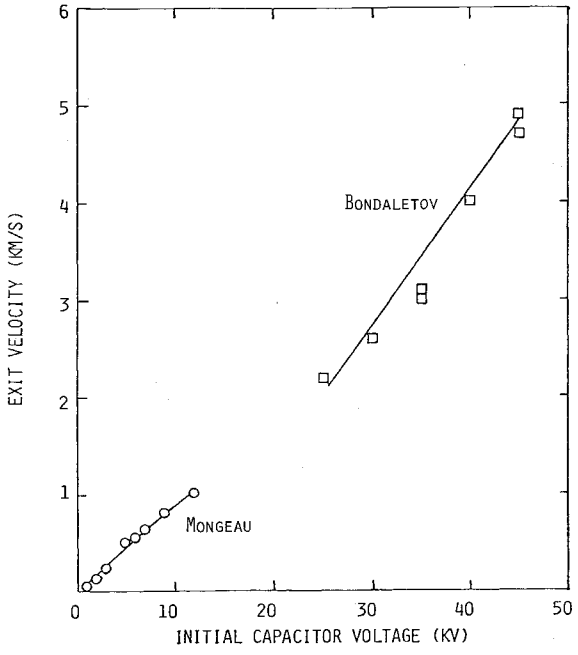

Fig. 2 Experimentally measured exit velocities as a function of initial capacitor voltage showing linear relationship.

by solving the circuit equations in the two current loops. For the driver circuit

$$V_c = R_0 I_1 + (L_0 + L_1)\frac{dI_1}{dt} + \frac{d(M_{12}I_2)}{dt} \tag{2}$$

where V_c is the voltage drop across the capacitor. Throughout this study L_0 was assumed to be 0.25×10^{-6} and R_0 to be 0.005Ω. The circuit equation for the reaction mass is identical except for the lack of the capacitor voltage drop

$$0 = I_2 R_2 + \frac{d(M_{12}I_1)}{dt} + \frac{dI_2}{dt} \tag{3}$$

The instantaneous capacitor voltage is found from

$$\frac{dV_c}{dt} = -\frac{I_1}{C} \tag{4}$$

Radial forces are also produced on the reaction mass. An inward radial force is induced in the reaction mass by the drive coil, however, this force is counteracted by the current induced in the reaction mass which acts on itself producing a force in the outward radial direction. The magnitude of the resultant sum of the forces was calculated and compared to the axial force where it was found that the reaction mass would be accelerated out of the coupling region before significant radial deformation could occur, even when the reaction mass is in the liquid state. The resistive heating of the reaction

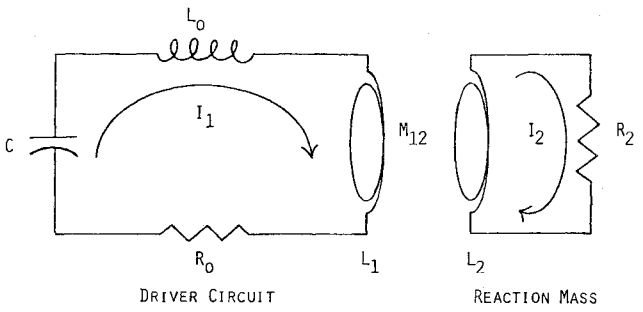

Fig. 3 Electrical model of pulsed inductive thruster/reaction-mass system.

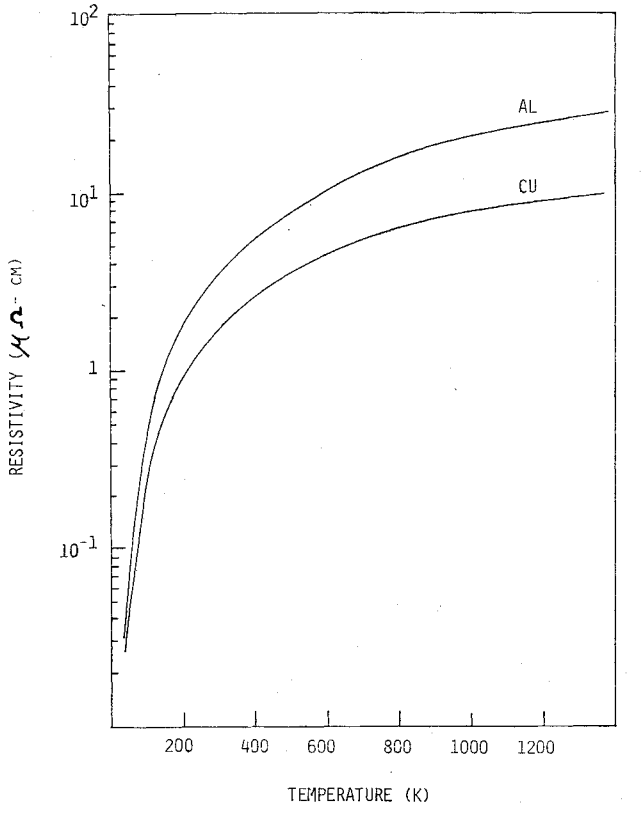

Fig. 4 Variation of resistivity with temperature for aluminum and copper showing sharp increases at low temperatures.

mass is described by

$$\frac{dT}{dt} = \frac{R_2 I_2^2}{C_p m} \tag{5}$$

It was assumed that the driver coil could be either passively or actively cooled in order to maintain a constant temperature.

In order to model thermal effects associated with resistive heating accurately, temperature-dependent values for the resistivity, specific heat, and density were used. Figure 4 plots the variation of resistivity with temperature for aluminum and copper,[6,7] showing the increase of resistivity with temperature, particularly in the low-temperature region. Figure 5 shows the specific heat of aluminum and copper as a function of temperature.[6] The energy required for the phase change of aluminum at its melting point is accounted for by the sharp increase in specific heat around its melting point. Finally, the density of liquid aluminum vs temperature was used as shown by Fig. 6.[8] All three curves were incorporated into the numerical code as subroutines containing experimentally measured data points in a look-up table and interpolating between table points. The system of the five ordinary differential equations [Eqs. (1-5)] was numerically integrated in time using

a fourth-order Runge-Kutta scheme. The integration was continued until the separation between the driver coil and reaction mass increased to a value where the electromagnetic coupling between the two coils approached zero and the reaction mass ceased accelerating. The velocity achieved by the reaction mass at that point was then considered to be its exit velocity.

Results

Temperature-Dependent Material Properties

The first effect examined was that of resistive heating combined with temperature-dependent reaction-mass material properties. Figure 7 compares the constant property analysis conducted by Mongeau[2] with the variable property analysis conducted by the authors for aluminum exhaust material. It was found early in this investigation that the use of aluminum instead of copper for the reaction mass resulted in a much higher exhaust velocity due to the lower density of aluminum even though its resistivity is higher than copper. It can be seen that the two analyses give identical results for initial capacitor voltages below 7.5 kV. Above 7.5 kV, the variable property analysis shows degraded performance due to lower reaction-mass current caused by increased electrical resistance. The increased resistance, is due, in turn, to a higher reaction-mass temperature caused by resistive heating. Both analyses approach linear behavior at high initial voltages although with different slopes.

Geometry

The geometry of the drive-coil/reaction-mass current loop system has a very strong effect on the mutual inductance, M_{12}, and the mutual inductance gradient, dM_{12}/dx, which influences both the induced currents and the resultant force. This study assumed that the reaction mass could pass through the center of the drive coil in order to permit repetitively pulsed operation. Thus, whenever a reaction-mass loop was sized, the driver coil was sized just large enough for the reaction mass to pass through its longitudinal axis. Drive-coil and reaction-mass diameters were of the order of 0.5-4.0 cm, as these small sizes were required to obtain high exit velocities with the metallic reaction masses. The resistance of the reaction mass is also a function of its geometry. Excluding thermal effects, the most efficient geometry is that where the ratio of the drive-coil and reaction-mass current loop radii is close to unity. Thus, for a given mass of exhaust material, a large radius would be preferred. However, the process of resistive

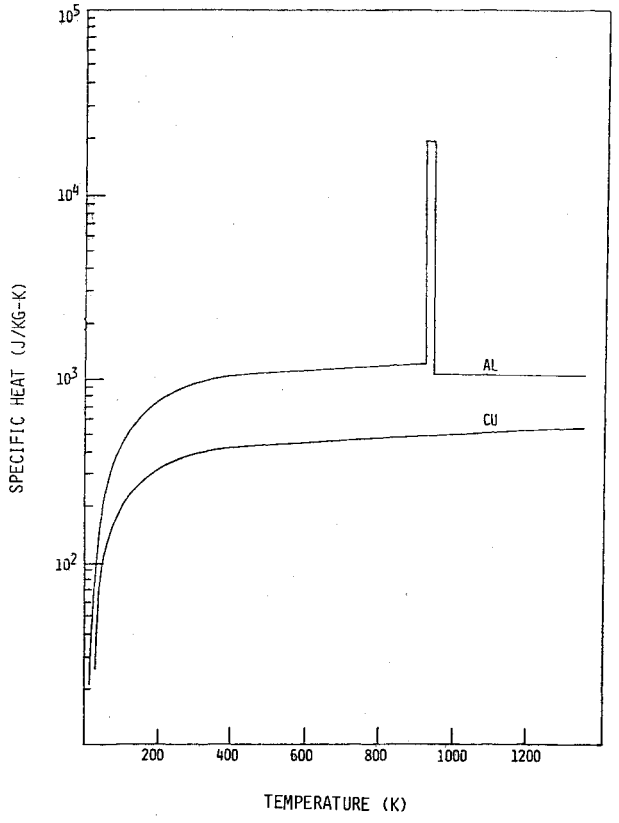

Fig. 5 Variation of specific heat with temperature for aluminum and copper. Large step for aluminum reflects solid- to liquid-phase change.

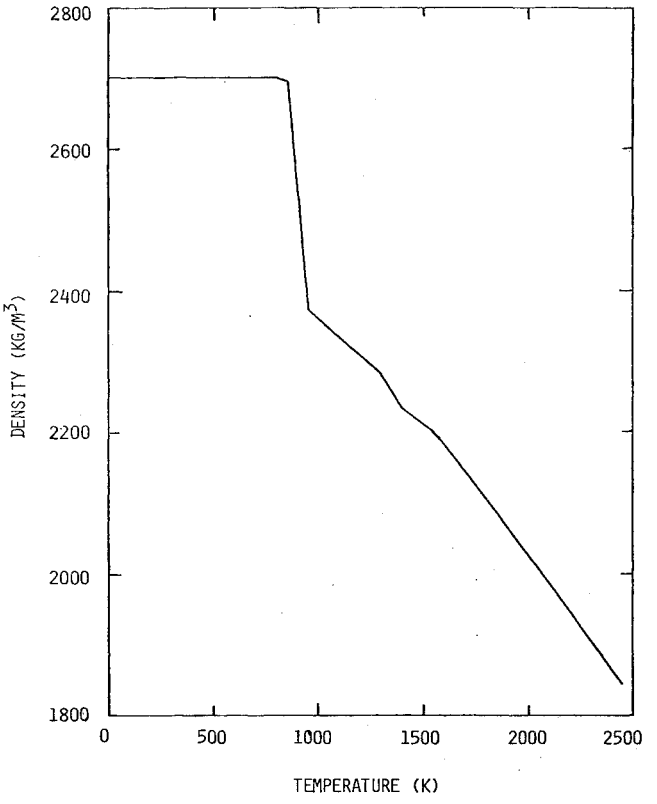

Fig. 6 Variation of density with tempeature for aluminum showing constant value for soild phase and decreasing values with temperature for liquid phase.

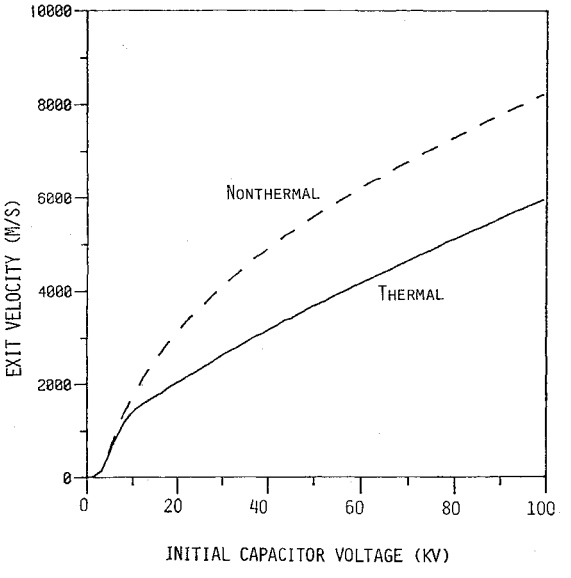

Fig. 7 Predicted exit velocities vs initial capacitor voltage for thermal and nonthermal analyses showing decreased performance due to thermal effects.

heating favors a small radius with its associated large current flow cross section since, for a fixed mass, as the radius decreases the cross-sectional area increases. Figure 8 shows that the cumulative effect of these two conflicting processes is to produce an optimum radius for the reaction-mass current loop. Exit velocity is plotted vs starting distance from the driver coil for three exhaust mass radii. The initial capacitor charge is 20 kV and the reaction mass is 0.2 g of aluminum. Similar behavior is observed for other exhaust material masses and initial capacitor voltages. It can be seen, however, from Fig. 8, that the exhaust velocity is not very sensitive to the reaction-mass radius near the optimal value.

Starting Location

The nonthermal analysis produces the highest exhaust velocity when the reaction mass is initially positioned an infinitesimal distance above the plane of the drive coil (if the two current loops are in exactly the same plane $dM_{12}/dx=0$ and no force is generated even though current will be induced in the reaction mass). However, the thermal analysis, quickly showed that an optimal starting location existed (Fig. 8). The reason for this is that the mutual inductance M_{12}, which governs the current induced in the reaction mass, is a maximum when the two current loops are in the same plane, designated by $x=0$ (Fig. 9). However, the mutual inductance gradient dM_{12}/dx, which determines the accelerating force produced, is a maximum when the current loops are a short distance apart. Thus, in the thermal analysis, a too-small initial separation results in a large amount of current being induced in the reaction mass before this current can generate a substantial accelerating force. However, this current can resistively heat the reaction mass, raising its resistance and thereby decreasing the current present when the reaction mass is in the region of maximum dM_{12}/dx, therefore decreasing the acceleration.

Storage Capacitance

The initial stored electrical energy is proportional to the capacitance. The thruster converts this stored energy into directed kinetic energy of the reaction mass. However, as Fig. 10 demonstrates, as the storage capacitance is increased from zero, the exhaust velocity first increases rapidly but eventually levels off such that an increase in capacitance will not increase the exit velocity.[1] The reason for such behavior is that the acceleration of the reaction mass moves it out of the interaction region with the driver coil, and any electrical energy remaining in the capacitor cannot be utilized. Four initial capacitor voltages are shown on Fig. 10, and it can be seen that, as the initial voltage is increased, the exhaust velocity levels out at smaller capacitance values. The figure also shows that the use of a 100-μF capacitor provides near-optimal performance for initial capacitor voltages greater than 20 kV.

Exhaust Material Mass

For a given amount of stored electrical energy, $CV_0^2/2$, there is an optimal mass for the exhaust material ring. A too-small mass will cause the exhaust ring to be accelerated out of the interaction region before all of the electrical energy can be transferred from the capacitor, while a too-large mass consumes all of the available electrical energy but is simply too massive to be accelerated to a high velocity. Figure 11 plots the exhaust velocity vs initial exhaust material temperature for several exhaust ring masses with an initial capacitor voltage of 50 kV. The figure shows that for this particular system, a mass of approximately four times the baseline mass, M_0, gives the highest exhaust velocities over the entire temperature range examined.

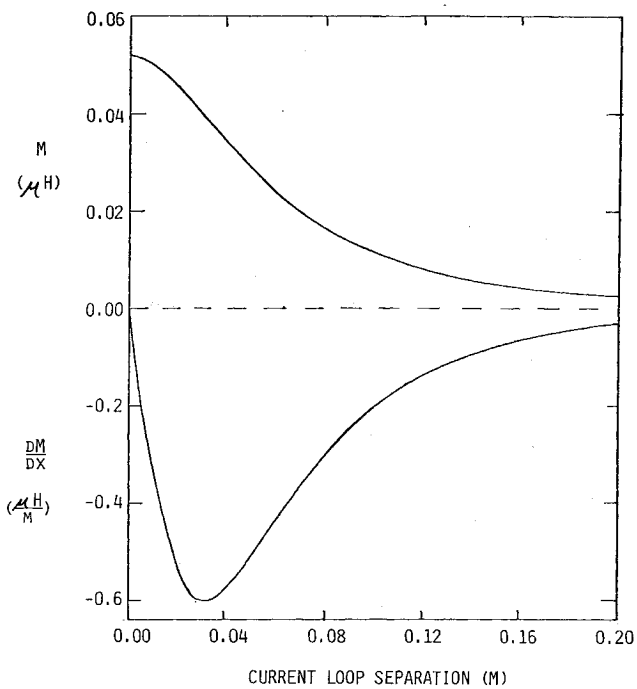

Fig. 9 Mutual inductance M and mutual inductance gradient dM/dx as a function of current loop separation for a representative geometry. M peaks at $x=0$, while the magnitude of dM/dx peaks at a nonzero separation.

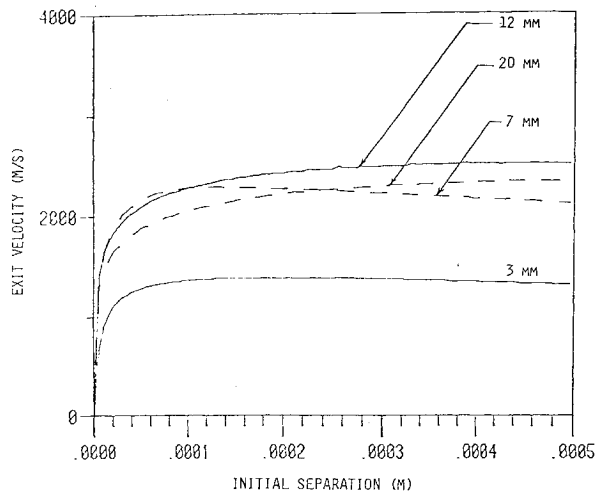

Fig. 8 Variation of predicted exit velocity as a function of initial current loop separation for four reaction-mass radii at constant mass.

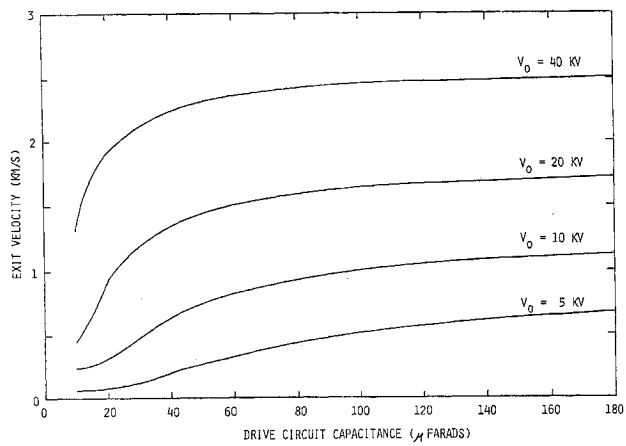

Fig. 10 Variation of predicted exit velocity as a function of drive circuit capacitance for four initial capacitor voltages showing asymptotic behavior.

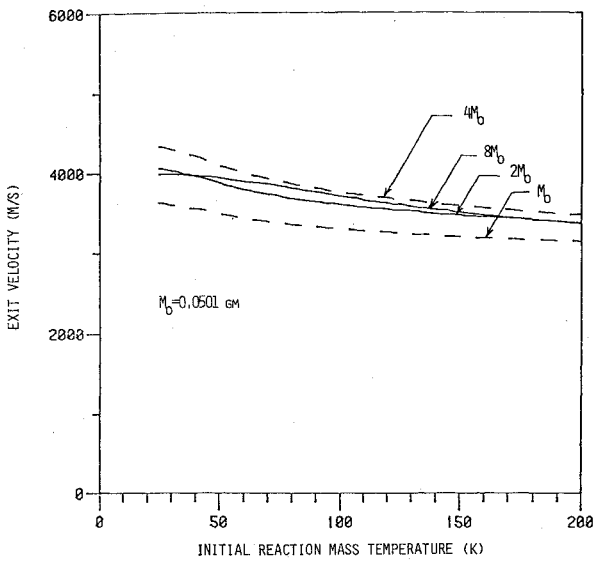

Fig. 11 Variation of predicted exit velocity as a function of initial reaction-mass temperature for four initial exhaust material masses showing an optimum mass and weak initial temperature dependence.

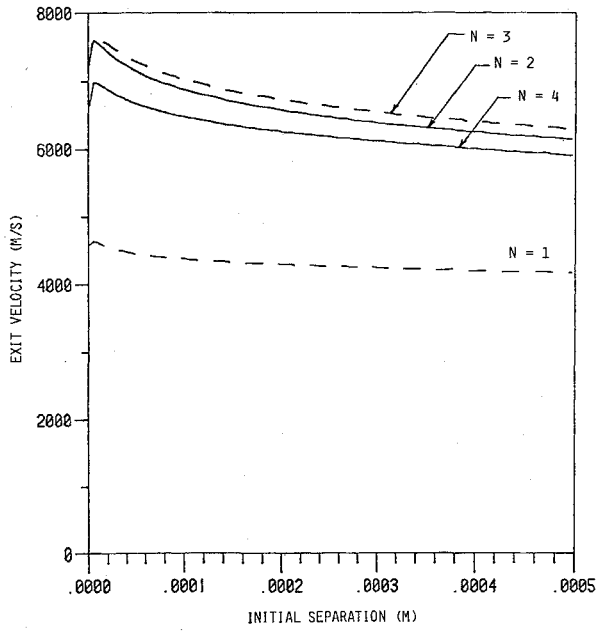

Fig. 12 Predicted exit velocity as a function of initial current loop separation for drive coils with from one to four coil turns showing optimal performance for a three-turn coil.

Exhaust Material Temperature

The electrical resistance of the reaction mass controls the amount of current induced in it and, therefore, the force available to accelerate it. Since the resistance is a function of temperature, it was anticipated that by cooling the reaction mass into the cryogenic region vastly increased exhaust velocities would be obtained. However, as shown in Fig. 11, reducing the reaction-mass initial temperature down to 25 K does not improve the exhaust velocity greatly. This is due to the decreased specific heat at low temperatures, causing the reaction mass to resistively heat itself very quickly even though the resistance is low. Cooling the reaction mass from 200 K down to 25 K only increased the exhaust velocity by approximately 25%.

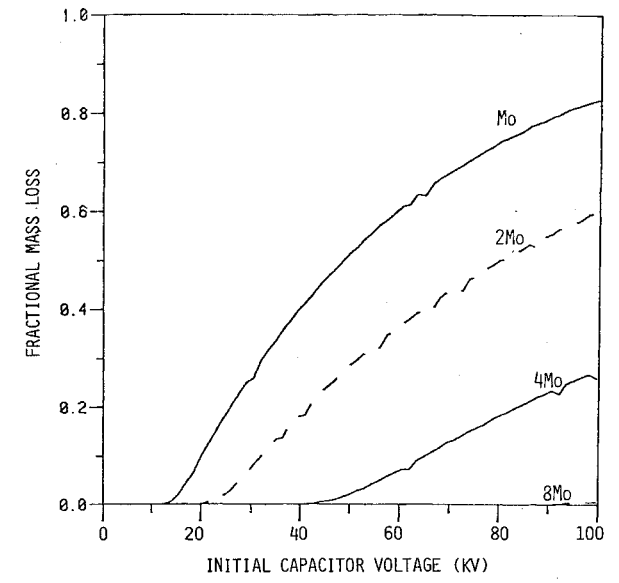

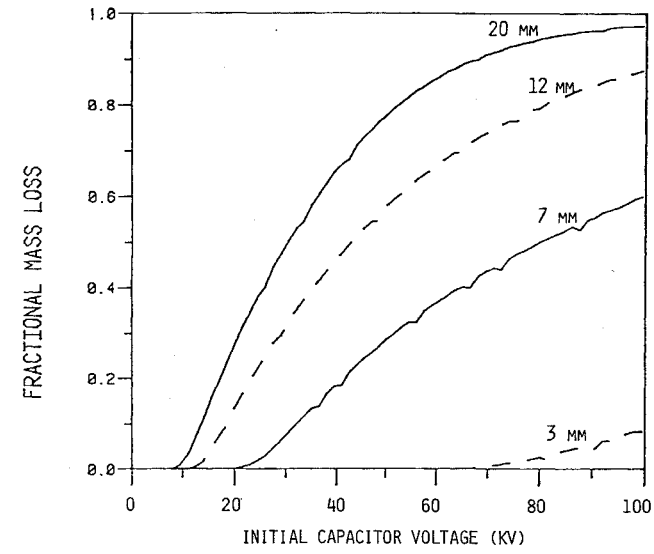

Fig. 13 Predicted fractional mass loss as a function of initial capacitor voltage for a) four initial exhaust material masses showing that small masses can be driven toward complete evaporation, and b) four reaction-mass radii at constant mass showing that a large-radius reaction mass can be driven toward complete evaporation.

Drive-Coil Loops

The current loop induced in the reaction mass will consist of a single loop but the number of loops in the drive coil can be controlled in an effort to enhance the mutual inductance M_{12} and the mutual inductance gradient dM_{12}/dx. Multilooped reaction masses were never considered due to the extreme difficulties one would encounter in attempting to manufacture them to the small size scales considered in this study. Figure 12 plots the exit velocity vs starting separation for a system where the only parameter varied is the number of drive-coil turns. Resutls for a drive coil with one to four loops are shown. It can be seen that for this system three loops of the drive coil are optimal, providing approximately a 50% improvement in exhaust velocity over a single-loop drive coil.

Reaction-Mass Evaporation

The state of the reaction mass once it is exhausted from the thruster is of concern due to potential space pollution problems. The thermal analysis showed that temperatures above the melting point of the reaction mass are easily obtained by

the resistive heating. Therefore, it was felt that some evaporation of the reaction mass would occur and, in fact, it may be desirable to drive all of the reaction mass to evaporation in order to avoid littering space with thousands of small metallic rings traveling at high velocities. Thus, the vacuum evaporation process for liquid metals was added to the numerical model with the mass of the exhaust material now being treated as another dependent variable. The evaporation rate as given by Dushman[9] is

$$\log W = P - 0.5\log\frac{T}{MW} - 4.234 \tag{6}$$

where W is the evaporation rate in g/cm^2-sec, P the vapor pressure of the reaction mass in microns of mercury, and MW the reaction-mass gram-molecular weight. The vapor pressure of liquid aluminum as a function of temperature was obtained by using Kubaschewski's vapor pressure equation[10]

$$\log P = \frac{-16450}{T} + 15.36 - 1.023\log T \tag{7}$$

Figure 13a shows the fractional reaction-mass loss as a function of initial capacitor voltage for several initial exhaust masses. A fractional mass loss of 1 means that the entire reaction mass has evaporated. It can be seen from the figure that for low initial capacitor voltages, no resistively driven evaporation occurs, but for high voltages, almost complete evaporation can take place. It is also shown that for fixed drive-coil and exhaust current loop radii, a smaller initial exhaust mass is more readily driven to evaporation because the exhaust current loop cross section is smaller, and, therefore, the initial resistance is higher, leading to faster heating. Figure 13b plots the fractional mass loss as a function of initial radii keeping mass constant. As the radius is increased, the decreased current loop cross section leads to a higher resistance and, therefore, greater resistive heating. Also, a larger radius gives more surface area for evaporation. Thus, for given exhaust material mass, conditions leading to complete evaporation can be obtained with the correct combination of initial capacitor voltage and reaction-mass geometry. In the same manner, conditions can be chosen to completely avoid evaporation.

Overall efficiencies were calculated, with the assumption that any electrical energy remaining in the drive circuit after the reaction mass leaves the acceleration region could be recovered. The overall efficiency was defined as the reaction-mass kinetic energy divided by electrical energy removed from the drive circuit. It was found that ohmic heating losses in the drive circuit were negligible, leaving the reaction-mass ohmic heating as the major loss mechanism. The calculations showed that the overall efficiency was a function of whether one chose to drive the reaction mass to complete evaporation or not. If a reaction-mass geometry was chosen to avoid heating to evaporation, the efficiency approached 100%, however, if the reaction mass was driven to near complete evaporation, overall efficiencies dropped below 33%.

Multiple Drive Coils

After single drive-coil configurations were examined, attention was focused on the possibility of utilizing multiple drive coils. The reaction mass would pass through each one sequentially, being accelerated by each drive coil in turn. Due to the fact that for a single drive coil the acceleration process is completed in a short distance (approximately the diameter of the drive coil), the provision was made to allow the drive coils to be located in proximity to each other and to electrically interact with each other through the mutual inductance. Each drive-coil system was modeled by the addition of a circuit loop equation similar to Eq. (2) but with a $d(MI)/dt$ term added for each additional drive coil. The resulting set of coupled ordinary differential equations was placed in matrix form and inverted prior to integration by the fourth-order Runge-Kutta scheme. The number of additional drive coils as well as the spacing could be controlled and each drive coil could be triggered separately, either at a predetermined time or with the reaction mass at a predetermined location. It was found, however, that additional drive coils improved performance no more than a few percent, i.e., two drive coils, each one connected to a capacitor charged to a 50-kV capacitor, produced an exit velocity only 3.2% higher than a single coil connected to a 50-kV capacitor. The reason for this is the $d(MI)/dt$ term in Eqs. (2) and (3). When expanded, this term becomes

$$\frac{d(MI)}{dt} = M\frac{dI}{dt} + I\frac{dM}{dt} = M\frac{dI}{dt} + I\frac{dM}{dx}\frac{dx}{dt} \tag{8}$$

The last term is called the "back emf" and is proportional to the reaction-mass velocity. In fact, as the reaction-mass velocity becomes large, this term takes a dominant role in Eqs. (2) and (3). Thus, the final exhaust velocity is a function of the maximum voltage available and adding drive coils with the same capacitor voltage does little to improve performance. The result is that if a certain capacitor charging voltage is available, it should be applied to a single drive-coil circuit.

Conclusions

A pulsed inductive electromagnetic thruster utilizing a solid conducting ring as the reaction mass was modeled. The analysis included the resistive heating of the reaction mass by the induced current, and the density, resistivity, and specific heat of the reaction mass were allowed to vary as functions of the temperature. Aluminum was used as the reaction mass throughout most of the analyses since its lower density produced a higher exit velocity than copper even though its resistivity is higher. It was found that the inclusion of the thermal analysis produced exit velocity predictions below those obtained from a nonthermal analysis. Thermal effects also created optimal geometries and starting separations for the reaction mass as a function of initial capacitor voltage and exhaust material mass. The effects of drive-coil circuit capacitance were examined with the conclusion that a value of 100 μF was a good choice for initial voltages above 20 kV and initial exhaust material mass on the order of grams. The initial temperature of the reaction mass was found to have a small effect on the exhaust velocity over the temperature range of 25-200 K. The vacuum evaporation process of the heated reaction mass was examined and found to be able to account for the complete evaporation of the reaction mass under certain circumstances. Increasing the number of drive-coil loops until an optimum was reached was found to greatly enhance the exhaust velocity, while the use of additional drive-coil circuits at the same or lower initial capacitor voltage did not increase the exit velocity. Out of all of the configurations examined, the highest predicted exhaust velocity for an initial capacitor voltage of 20 kV was 4000 m/s (equivalent to a specific impulse of 400 s), while for an initial capacitor voltage of 50 kV, 7500 m/s was obtained.

Acknowledgments

This work was sponsored by the Air Force Office of Scientific Research under Grant AFOSR-82-0196, Amendment A. Thanks are extended to Dr. Peter Mongeau for several fruitful conversations.

References

[1]Lovberg, R. H. and Dailey, C. L., "Large Inductive Thruster Performance Measurement," *AIAA Journal*, Vol. 20, July 1982, pp. 971-977.

[2]Mongeau, P., "Single Stage Pulsed Induction Reaction Engine," AIAA Paper 81-0752, April 1981.

[3]Mongeau, P. and Kolm, H., "Metallic Induction Reaction Engine," AIAA Paper 82-1279, June 1982.

[4]Mongeau, P. P., "Coaxial Air Core Electromagnetic Accelerator," Ph.D. Thesis, Department of Physics, Massachusetts Institute of Technology, Cambridge, MA, 1981.

[5]Bondaletov, V. N. and Ivanov, E. N. "Ultrahigh Axial Acceleration of Conducting Rings," *Soviet Physics, Technical Physics*, Vol. 22, Feb. 1977, pp. 232-234.

[6]Hodgman, C. D., ed., *Handbook of Chemistry and Physics*, The Chemical Rubber Publishing Co., Cleveland, OH, 1961.

[7]Meaden, G. T., *Electrical Resistance of Metals*, Plenum Press, New York, 1965.

[8]Wilson, R. P. Jr., "The Density of Aluminum at 2450-2900 K," *High Temperature Science*, Vol. 1, 1969, pp. 267-372.

[9]Dushman, S., *Scientific Foundations of Vacuum Technique*, John Wiley & Sons, New York, 1949, pp. 740-752.

[10]Maissel, L. I. and Glang, R., eds., *Handbook of Thin Film Technology*, McGraw-Hill Book Co., New York, 1970, pp. 12-14.